Research on Obstacle Avoidance of Redundant Robots Based on Geometric Models

Yu Liu, Bin Liang, Kui Sun
Research Academy of Science and Technology
Harbin Institute of Technology
Shenzhen, Guangdong Province, China
lyu11@hit.edu.cn

Yanshu Jiang
School of Automation
Harbin Science and Technology University
Harbin, Heilongjiang Province, China
jiangyanshu@yahoo.com.cn

***Abstract*- The paper directs the mathematical models of the sphere and the column obstacles for a redundant robot, which can be looked on as a reference for other complex shaped obstacles. Based on the models, the performance criterion function of obstacle avoidance is presented in light of artificial potential field method. Subsequently, through optimizing the performance criterion the simulation of obstacle avoidance is studied. At last, the experiment of obstacle avoidance of a 7-DOF redundant robot is carried out, which verifies the validity of the built models.**

I. INTRODUCTION

The prominent advantage of the redundant robot is to be capable of completing some extra tasks in complex environments through optimizing redundant degree of freedoms. For example, in order to paint an automobile's driving room inside, the robot's end effector is not only required to move in a certain trajectory, but also the link of the robot can not collide with the automobile body, which is difficult to an ordinary industrial robot. However, a redundant robot can reach the aim by building the performance criteria function of collision avoidance and optimizing the joints' trajectories easily.

At present, the obstacle avoidance of the redundant robot can be divided into four categories generally.

1) Obstacle avoidance based on the geometrical model.
2) Obstacle avoidance based on the range-finder sensor.
3) Obstacle avoidance based on vision.
4) Hybrid obstacle avoidance based on the previous three methods.

Obstacle avoidance based on the geometrical model mainly aims to the fixed obstacles. Firstly, we need to build a mathematical model according to the obstacle shape, and then construct a performance criterion function, at last, through optimizing the function the redundant robot can avoid the obstacle. Typically, by approximating the obstacle and robot link into polyhedrons described by the nodes and calculating the distances among the nodes, Chi Youn Chung [1] realized the robot link's obstacle avoidance based on the gradient projection algorithm. Seiji Aoyagi and Kazuya Tashiro **[2] assumed the models of six elementary types of obstacles, taking account of real environment.** Hisashi Sugiura etc [3] used the geometrical modeling method for **the humanoid** robot ASIMO to realizing real-time self collision avoidance.

To a moving or rotating obstacle randomly, obviously the mathematical models of the fixed obstacles will not be adapted to solve the problems. Generally, in these instances, obstacle avoidance based on range finder sensors or vision will work it. Utilizing the capacitance sensor arranged on the robot link, Novak and Feddema [4] realized to proportionally reduce the input speed in the perpendicular direction between the sensors and obstacles according to its readings. Woong-Jang Cho and Dong-Soo Kwon [5] simulated a sensor-based obstacle avoidance in an unstructured environment for a redundant manipulator using a velocity potential function.

Okada [6] carried out the path planning based on visual servo, and then achieved collision avoidance combined with the self- organizing neural network.

The hybrid collision avoidance method also attracts some researcher and makes great progress, typically, for example, the artificial potential field method [7,8].

II. MODEL OF COLLISION AVOIDANCE

The fixed geometrical obstacle is the most familiar one, and building the collision-avoidance model is simple, handy and practical. However, the form of the obstacle is complex, so the model that represents the obstacles is impossible to contain all objects. Here, only the spherical obstacle and the cylindrical obstacle are modeled precisely while other entities (for example, cuboid, pyramid and cone) are done according to the two modeling methods. Here, for simplicity, the redundant robot links are considered as the column.

A. Model of Spherical Obstacles

As shown in Fig.1, the redundant robot consists of two parts, namely the upper arm *SE* and the forearm *EW*, here, the points *S*, *E* and W are respectively the shoulder point, the elbow point and the wrist point, the right-hand coordinate frame's origin *O* overlaps with S, the center of the spherical surface lies in the point O_1, the distances from the point O_1 to the upper arm and the forearm are respectively $d_1$and d_2, the perpendicular points are respectively D_1 and D_2, and the spherical radius is *r*. The end effector's collision avoidance is realized through path-planning, here it is not considered. In the Fig. 1, the coordinates of the points *E* and *W* are easy to be evaluated. Supposed that coordinates of the points *E* and *W*

1-4244-2386-6/08/$20.00 ©2008 IEEE

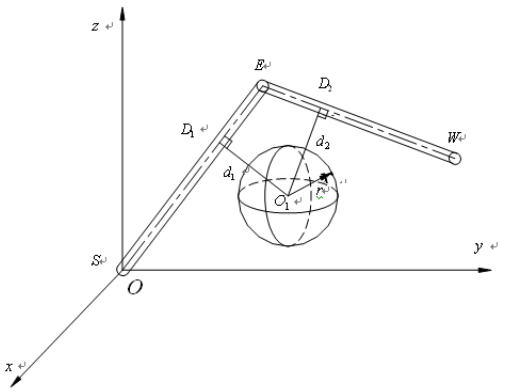

Fig. 1 Model of spherical obstacle

equation of *SE* and *EW* are respectively written as:

$$SE:\ \frac{x}{x_e}=\frac{y}{y_e}=\frac{z}{z_e}$$

$$EW:\ \frac{x-x_e}{x_w-x_e}=\frac{y-y_e}{y_w-y_e}=\frac{z-z_e}{z_w-z_e}$$

The shortest distances from the spherical surface to the upper arm and the forearm are respectively assumed d_u and d_f. Before calculating d_u and d_f, we need to judge if the perpendicular points D_1 and D_2 are respectively located on the linear segment *SE* and *EW*. According to the different cases the discussion follows.

1. The points D_1 and D_2 are respectively located on the linear segment *SE* and *EW*, so according to the distance calculation formula between two points, d_1 is easy to be evaluated.

$$d_1=\sqrt{(x_0-x_{D1})^2+(y_0-y_{D1})^2+(z_0-z_{D1})^2}$$

Similarly, d_2, *OE* and *OW* can be done. Then, d_u and d_f are calculated as follows.

$$d_u=d_1-r-r_0 \quad d_f=d_2-r-r_0 \tag{1}$$

Where r_0 is the cylindrical radius of the redundant robot links. If the point D_1 is located on the line segment *SE*, the following formula must be satisfied.

$$0\le x_{D1}\le x_e$$

Similarly, the point D_2 is also.

2. The point D_1 is located on the line segment *SE*, but the point D_2 is located on the extended line of the line segment *EW*. Then d_u and d_f are calculated as follows.

$$d_u=d_1-r-r_0 \quad d_f=OW-r \tag{2}$$

3. The point D_2 is located on the line segment *EW*, but D_1 is located on extended line of the line segment *SE*, Then only d_f need to be calculated as follows.

$$d_f=d_2-r-r_0 \tag{3}$$

4. The points D_1 and D_2 are respectively located on the extended lines of the line segments *SE* and *WE*, then the shortest distance from the spherical surface to the robot link is not d_u and d_f, but it is O_1E-r-r_0, which is written as:

$$d=O_1E-r-r_0 \tag{4}$$

Until now, the mathematical model of the spherical obstacles is obtained.

B. Model of Cylindrical Obstacles

Comparatively, the mathematical model of cylindrical obstacles is more complex, and here only a few typical examples are discussed.

As shown in Fig. 2, the *o-xyz* right-hand coordinate frame is built, whose origin is the same as the shoulder point *S*. Not losing generality, the nether surface of the column is located in the plane *oxy*, its axis O_1O_2 is parallel to the axis *z* and respectively intersects the nether and above surfaces of the column at the points O_1: (x_1, y_1, z_1) and O_2: (x_2, y_2, z_2). The axis O_1O_2, the Upper arm *SE* and the forearm *EW* are assumed to be non-coplanar, O_3D_1 is the common normal between the link *SE* and the axis O_1O_2, and the perpendicular points are respectively D_1 and O_3, d_1 denotes O_3D_1. Correspondingly, O_4D_2 is the common normal between the link *EW* and the axis O_1O_2, and the perpendicular points are respectively D_2 and O_4, d_2 denotes O_4D_2. The

Supposed that the point O_1 coordinate is (x_0, y_0, z_0), according to spatial analytical theory, the points D_1 and D_2 coordinates D_1: (x_{D1}, y_{D1}, z_{D1}) and D_2: (x_{D2}, y_{D2}, z_{D2}) can respectively be solved as follows.

where $x_{D1}=\dfrac{x_e^2x_0+x_ey_ey_0+x_ez_ez_0}{x_e^2+y_e^2+z_e^2}$

$$y_{D1}=\frac{y_e^2y_0+x_ey_ex_0+y_ez_ez_0}{x_e^2+y_e^2+z_e^2}$$

$$z_{D1}=\frac{z_e^2z_0+x_ez_ex_0+y_ez_ey_0}{x_e^2+y_e^2+z_e^2}$$

$$x_{D2}=x_e+\frac{(x_w-x_e)((x_w-x_e)(x_0-x_e)+(y_w-y_e)(y_0-y_e)+(z_w-z_e)(z_0-z_e))}{(x_w-x_e)^2+(y_w-y_e)^2+(z_w-z_e)^2}$$

$$y_{D2}=y_e+\frac{(y_w-y_e)((x_w-x_e)(x_0-x_e)+(y_w-y_e)(y_0-y_e)+(z_w-z_e)(z_0-z_e))}{(x_w-x_e)^2+(y_w-y_e)^2+(z_w-z_e)^2}$$

$$z_{D2}=z_e+\frac{(z_w-z_e)((x_w-x_e)(x_0-x_e)+(y_w-y_e)(y_0-y_e)+(z_w-z_e)(z_0-z_e))}{(x_w-x_e)^2+(y_w-y_e)^2+(z_w-z_e)^2}$$

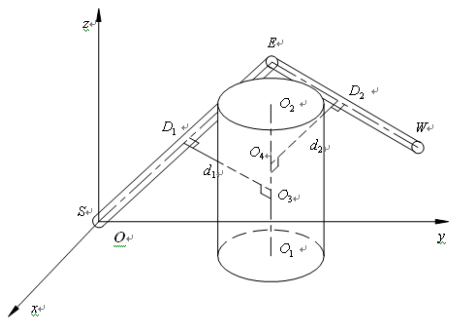

Fig. 2 Geometrical model 1 of the cylindrical obstacle

geometrical equations of the column side surface are assumed as follows.

$$\begin{cases}(x-x_1)^2+(y-y_1)^2=r^2\\ 0\le z\le z_2\end{cases} \tag{5}$$

Where r is the radius of the column, the line O_1O_2 equation is

$$\begin{cases}x=x_1\\ y=y_1\end{cases} \tag{6}$$

$$x_{D2}=\frac{(x_w-x_e)(y_1y_w-y_1y_e+x_1x_w-x_1x_e-y_ey_w+y_e^2)+x_e(y_w-y_e)^2}{(y_w-y_e)^2+(x_w-x_e)^2}$$

$$y_{D2}=\frac{(y_w-y_e)(y_1y_w-y_1y_e+x_1x_w-x_1x_e-x_ex_w+x_e^2)+y_e(x_w-x_e)^2}{(y_w-y_e)^2+(x_w-x_e)^2}$$

$$z_{D2}=\frac{(z_w-z_e)((y_1-y_e)(y_w-y_e)+(x_1-x_e)(x_w-x_e))}{(y_w-y_e)^2+(x_w-x_e)^2}+z_e=z_4$$

Based on the above formula， d_1 and d_2 can be calculated easily. If $O_3\in O_1O_2$, $O_4\in O_1O_2$, $D_1\in SE$ and $D_2\in EW$ are assumed, d_u and d_f are calculated as follows.

$$d_u=d_1-r-r_0 \quad d_f=d_2-r-r_0 \tag{7}$$

Subsequently, another geometrical relation between the column and the redundant robot is discussed, namely O_3 and O_4 are on the extended line of the line segment O_1O_2 , other conditions are the same as the previous ones.

As shown in Fig 3, the plane constructed by *SE* and *EW* intersects the circle on the above surface of the column at the points *A* and *B* respectively. The lines AD_3 and BD_4 are respectively perpendicular to the links *SE* and *EW* at the points D_3.and D_4. In the configuration, the links *SE* and *EW* of the redundant robot are the most likely to collide with the contour circle of the above surface of the column, namely the points *A* and *B* are dangerous points. The coordinates of the points *A* and *B* respectively follows.

$$(x_A,y_A,z_A)\quad(x_B,y_B,z_B)$$

The circle equation of the above surface of the column is given by

$$\begin{cases}(x-x_1)^2+(y-y_1)^2=r^2\\ z=z_2\end{cases} \tag{8}$$

Its direction vector is $\vec{l}_{O_1O_2}=\{0,0,1\}$.

Subsequently, based on the spatial analytical geometry theory, from the above known condition we easily calculate the points D_1, D_2, O_3 and O_4 coordinates.

$$D_1:\ (x_{D1},y_{D1},z_{D1})\quad D_2:\ (x_{D2},y_{D2},z_{D2})$$

$$O_3:\ (x_3,y_3,z_3)\quad O_4:\ (x_4,y_4,z_4)$$

The solving processes are omitted here.

$$x_3=x_1\quad y_3=y_1$$

$$x_{D1}=\frac{x_e(x_1x_e+y_1y_e)}{x_e^2+y_e^2}$$

$$y_{D1}=\frac{y_e(x_1x_e+y_1y_e)}{x_e^2+y_e^2}$$

$$z_{D1}=\frac{z_e(x_1x_e+y_1y_e)}{x_e^2+y_e^2}=z_3$$

$$x_4=x_1\quad y_4=y_1$$

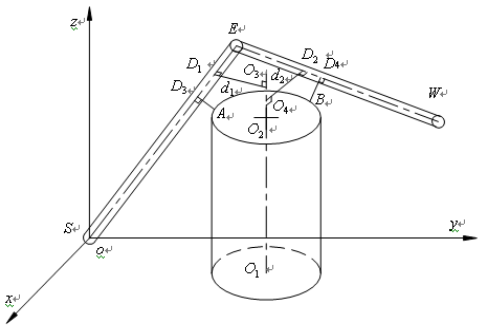

Fig. 3 Geometrical model 2 of the cylindrical obstacle

The plane equation through the points *S*, *E* and *W* is written as

$$cx+dy+ez=0 \tag{9}$$

The factors *c*, *d* and *e* can be evaluated through cross product between the two link vectors *SE* and *EW*.

$$\begin{bmatrix}c\vec{i}\\ d\vec{j}\\ e\vec{k}\end{bmatrix}=\begin{vmatrix}\vec{i}&\vec{j}&\vec{k}\\ x_e&y_e&z_e\\ x_w-x_e&y_w-y_e&z_w-z_e\end{vmatrix} \tag{10}$$

The combination of the Eqs. (8), (9) and (10) yield

$$x_A = (x_1cd^2 - dy_1c^2 - d(c^2(-2x_1cdy_1 - 2y_1z_2ed - d^2y_1^2 + d^2r^2 - 2x_1cez_2 - x_1^2c^2 - e^2z_2^2 + r^2c^2))^{1/2} - ez_2c^2)/(c(d^2 + c^2))$$

$$y_A = -(x_1cd - y_1c^2 + z_2ed - c(-2x_1cdy_1 - 2y_1z_2ed - d^2y_1^2 + d^2r^2 - 2x_1cez_2 - x_1^2c^2 - e^2z_2^2 + r^2c^2)^{1/2}/(d^2 + c^2)$$

$$z_A = z_2$$

$$x_B = (x_1cd^2 - dy_1c^2 + d(c^2(-2x_1cdy_1 - 2y_1z_2ed - d^2y_1^2 + d^2r^2 - 2x_1cez_2 - x_1^2c^2 - e^2z_2^2 + r^2c^2))^{1/2} - ez_2c^2)/(c(d^2 + c^2))$$

$$y_B = -(x_1cd - y_1c^2 + z_2ed + c(-2x_1cdy_1 - 2y_1z_2ed - d^2y_1^2 + d^2r^2 - 2x_1cez_2 - x_1^2c^2 - e^2z_2^2 + r^2c^2)^{1/2}/(d^2 + c^2)$$

$$z_B = z_2$$

Where $c = y_e(z_w - z_e) - z_e(y_w - y_e)$

$d = z_e(x_w - x_e) - x_e(z_w - z_e)$

$e = x_e(y_w - y_e) - y_e(x_w - x_e)$

So, we can easily evaluate the coordinates of the points D_3 and D_4 according to the coordinates of the above points A and B.

D_3: (x_{D3}, y_{D3}, z_{D3}) D_4: (x_{D4}, y_{D4}, z_{D4})

Accordingly, AD_3 and BD_4 can be represented by explicit formulas, so d_u and d_f are calculated as follows.

$$d_u = AD_3 - r - r_0 \quad d_f = BD_4 - r - r_0 \tag{11}$$

If $O_3 \in O_1O_2$ are assumed, and O_4 are on the extended line of the line segment O_1O_2, d_u and d_f will be calculated as follows.

$$d_u = d_1 - r - r_0$$

$$d_f = BD_4 - r - r_0 \tag{12}$$

Similarly, if $O_4 \in O_1O_2$ are assumed, and O_3 are on the extended line of the line segment O_1O_2, d_u and d_f will be calculated as follows.

$$d_u = AD_3 - r - r_0$$

$$d_f = d_2 - r - r_0 \tag{14}$$

Subsequently, the third geometrical relation between the column and the redundant robot, namely D_1 and D_2 are respectively on the extended line of line segment SE and WE, is discussed. As shown in Fig. 4, not losing generality, O_1O_2 is parallel to the axis y, ED is perpendicular to O_1O_2 at the point D, and other conditions are the same as the previous two cases. It can be seen that the point E is the dangerous point. Because the straight-line equation O_1O_2 and the coordinate of the point E are known, ED can be easily evaluated and d_u and d_f can be calculated as follows.

$$d_u = d_f = ED - r - r_0 \tag{15}$$

Until now, we largely have given a general discussion on the mathematical model of the cylindrical obstacle.

C. Performance Criterion Function Based on Collision Avoidance Models

According to general understandings, when the redundant robot links approach the obstacles to the bound of defined threshold values, the joints' trajectories of the redundant robot can be optimized to change the joint configuration and meet the requirements of collision avoidance. Before optimization we need build the performance criteria function of collision avoidance. Based on the theory of artificial potential fields, the following performance criteria function of collision avoidance for the upper arm is presented.

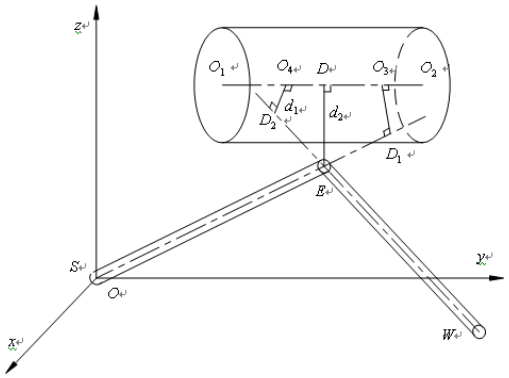

Fig. 1 Geometrical model 3 of the cylindrical obstacle

$$H_{pu} = \begin{cases} k_p(d_u - \lambda)^2 & d_u \le \lambda \\ 0 & d_u > \lambda \end{cases} \tag{16}$$

Where, k_p is a positive proportional factor, λ is the assumed threshold value for collision avoidance.

According to the above performance criteria function, it is easily found that if d_u equals to λ, H_{pu} will become minimum, and is the minimum value of the artificial potential energy. So, the problem of collision avoidance for the redundant robot is changed into optimization problem of the function H_{pu}. Similarly, the performance criteria function H_{pf} of collision avoidance for the forearm can be attained.

III. Simulation of Obstacle Avoidance

Considering complexity of calculation, we only choose the spherical obstacle as the simulated model, besides we choose the general gradient projection algorithm as the optimization method, the formula follows.

$$\dot{\vec{\theta}} = J^+\dot{\vec{x}} + k(I - J^+J)\vec{v} \tag{17}$$

The two performance criteria functions of the above upper arm and forearm divided, so they can not be optimized at the same time. Now through the weighing method we can build a united performance function as follows.

$$H_p = H_{pu} + 0.8H_{pf} \quad (17)$$

In this example, we adopt the 7-DOF redundant robot, whose D-H parameters are seen in Table I. The initial conditions are supposed as follows.

TABLE I
D-H PARAMETERS OF THE REDUNDANT ROBOT

Link i	θ_i (°)	α_i (°)	d_i(mm)	a_i(mm)
1	0	-90°	0	0
2	90°	90°	103.5	0
3	90°	0	0	262
4	90°	90°	0	0
5	0	-60°	363	0
6	0	60°	0	0
7	0	0	0	0

1. The initial joint angle vector is constructed as follows

$$\bar{\theta} = [0, \pi/10, 9\pi/10, \pi/6, 0, \pi/2, 0]^T$$

2. The end effector's speed vector is constructed as follows

$$v = \dot{x}(t) = [20, 0, -50, 0, 0, 0]^T \text{ (mm/s)}$$

3. Simulation period: 5ms; Simulation time: 2s.
4. The coordinate of the spherical center is assumed as (-230, 170, -100) (unit: mm) with respect to the base coordinate frame and the radius of the sphere is 100mm.
5. The threshold values are assumed as 250mm.

The simulation results are shown in Fig. 5. Here, u_1 and f_1 respectively denote the variable distance curves from the spherical center to the upper arm and the forearm without consideration of obstacle avoidance and only with the minimum joint angle norm, conversely, u_2 and f_2 do them under the condition of the optimization of collision avoidance, it can be easily seen that in the initial phases the two distance curves climb quickly and gradually trends to smoothness, which means nearer the redundant robot is from the obstacle, greater the optimization power is. When it continually goes farther away from the spherical obstacle, optimization power

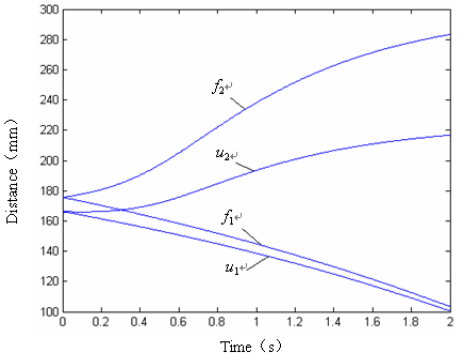

Fig. 5 Simulation of Collision Avoidance

becomes smaller. If the optimized distance functions are greater than the assumed threshold value, the optimization of collision avoidance will not be executed, which makes the redundant resource of the robot distributed more reasonably. Obviously, in the example, the redundant robot not only completes the main task (the above known condition 2), but also it performs the extra task, which makes the robot keep away from the spherical obstacle. Conversely, we see that the distance curves u_1 and f_1 decline rapidly, which means the robot links will approach to the spherical obstacle nearer and nearer and at last possibly collide with it.

So, it shows that using the above built models of collision avoidance the redundant robot can escape the obstacles through optimization of the joint trajectories, while in an complex environment without optimization a destructive mechanical interference may occur. Obviously, compared with a general robot, the redundant robot increases the dexterity of path-planning with the aid of the extra joints and improves the ability of performing the task.

IV. EXPERIMENT OF OBSTACLE AVOIDANCE

Subsequently, with experiment we will verify the ability of obstacle avoidance for the redundant robot. Here, simply, the spherical obstacle is replaced by a soft balloon. The computational flowchart of obstacle avoidance is shown in Fig. 6. The initial conditions of the experiment are given as follows

1. The initial joint angle vector is constructed as follows

$$\bar{\theta} = [0, \pi/5, 5\pi/6, \pi/6, 0, \pi/2, 0]^T$$

2. The end effector's speed vector is constructed as follows

$$v = \dot{x}(t) = [30, 0, -70, 0, 0, 0]^T \text{ (mm/s)}$$

3. Simulation period: 5ms; Simulation time: 4s.
4. The coordinate of the balloon center is assumed as (-230, 170, -100) (unit: mm) with respect to the base coordinate frame and the radius of the balloon is 100mm.
5. The threshold values are assumed as 250mm.

As shown in Fig. 7(a), with the above algorithm of obstacle avoidance the redundant robot is far from the soft balloon, conversely, without optimization of obstacle avoidance and only with the minimum joint angle norm the upper arm of the redundant robot collides with it, as shown in Fig. 7(b), which further proves rightness of the above model of collision avoidance and presents the flexibility of the redundant robot. By constructing the optimization functions, the redundant robot can carry out the more complicated tasks.

V. CONCLUSION

Aiming to the fixed geometrical obstacles (the sphere and the column), the paper gives some mathematical modeling methods. To the obstacles of other shape, the mathematical model can be derived similarly. Then based on the artificial potential field method we build the performance criteria function of obstacle avoidance. At last, as an illustration, we utilize the 7-DOF redundant robot developed by ourselves to carry out the simulation and experiment of obstacle avoidance. The results show that under the condition of fixed obstacles the performance criteria function of collision avoidance built with geometrical methods is simple and effective, but beyond doubt, the diversity of the obstacles increase the complexity of building the obstacle model. However, to a simpler and decided environment the method

of obstacle avoidance is feasible obviously.

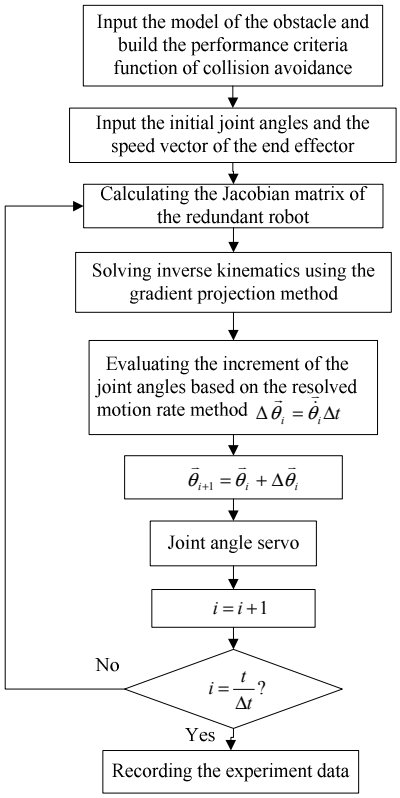

Fig. 6 Flowchart of collision avoidance for the redundant robot

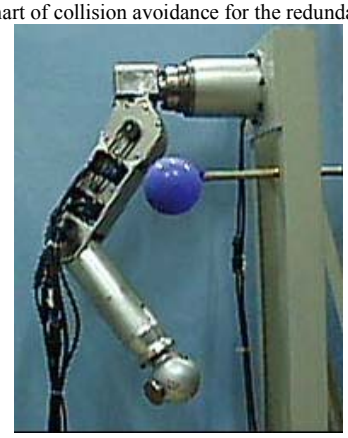

a)

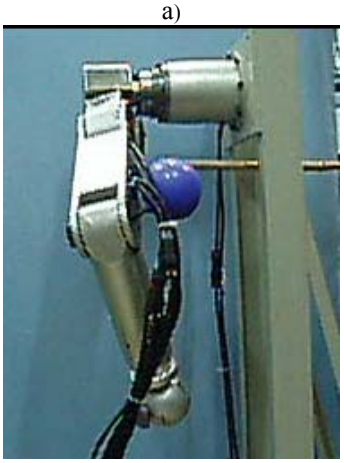

b)

Fig. 7 Collision with the balloon for the redundant robot

ACKNOWLEDGEMENT

The research is supported by National Natural Science Foundation of China (No.60775049).

REFERENCES

[1] Chi Youn Chung, Boom Hee Lee and Jung Hoon Lee, **"**Obstacle avoidance for kinematically redundant robots using distance algorithm," *in Proceedings of IEEE International Conference on Robots and Systems, Grenoble，France,* 1997, pp. 1787-1793

[2] Seiji Aoyagi, Kazuya, "Development of redundant robot simulator for avoiding arbitrary obstacles based on semi-analytical method of solving inverse kinematics," *in Proceedings of IEEE/RSJ International Conference on Intelligent Robots and Systems*, *San Diego,* 2007, pp. 3497- 3502

[3] Hisashi Sugiura, Michael Gienger, Herbert Janssen and Christian Goerick, "Real-time self collision avoidance for humanoids by means of nullspace criteria and task intervals," *6th IEEE-RAS International Conference, Genova, Italy*, 2006, pp. 575-880

[4] J.L. Novak, I.T. Feddema, "A capacitance-based proximity sensor for whole arm obstacle avoidance," *in Proceedings of IEEE International Conference on Robotics and Automation, Nice,* 1992, pp. 1307-1314

[5] Woong-Jang Cho**,** Dong-Soo Kwon, "Sensor-based obstacle avoidance for a redundant manipulator using a velocity potential function," *in Proceedings of IEEE International Conference on Robot and Human Communication, Seoul, South Korea,* 1996, pp. 306-310

[6] N. Okada, K. Minamoto and E. Kondo, "Collision Avoidance for a Visuo-motor System with a Redundant Manipulator Using a Self-organizing Visuo-motor Map," *in Proceedings of IEEE International Conference on Assembly and Task Planning, Fukuoka，Japan,* 2001, pp. 104 -109

[7] S.Higashi, S. Komada, M. Ishida and T. Hori, "Obstacle avoidance of redundant manipulators on visual servo system using estimated image features," *5th International Workshop on Advanced Motion Control,* Coimbra, 1998, pp. 165-170

[8] T. Laliberte, C.M. Gosselin, "Efficient algorithms for the trajectory planning of redundant manipulators with obstacle avoidance," *in Proceedings of IEEE International Conference on Robotics and Automation, San Diego,* 1994, pp. 2044-2049